

## Group-4 $\eta^1$ -Pyrrolyl Complexes Incorporating *N,N*-Di(pyrrolyl- $\alpha$ -methyl)-*N*-methylamine

Yahong Li, Angie Turnas, James T. Ciszewski, and Aaron L. Odom\*

Department of Chemistry, Michigan State University, East Lansing, Michigan 48824

Received August 13, 2002

Syntheses and properties of group-4 complexes incorporating the tridentate, dianionic ligand *N,N*-(dipyrrolyl- $\alpha$ -methyl)-*N*-methylamine, dpma, have been investigated. Addition of 1 equiv of H<sub>2</sub>dpma to Ti(NMe<sub>2</sub>)<sub>4</sub> and Zr(NMe<sub>2</sub>)<sub>4</sub> results in transamination with 2 dimethylamides providing Ti(NMe<sub>2</sub>)<sub>2</sub>(dpma) and Zr(NMe<sub>2</sub>)<sub>2</sub>(NHMe<sub>2</sub>)(dpma), respectively. Addition of 2 equiv of H<sub>2</sub>dpma to Zr(NMe<sub>2</sub>)<sub>4</sub> and Hf(NMe<sub>2</sub>)<sub>4</sub> results in production of the homoleptic complexes Zr(dpma)<sub>2</sub> and Hf(dpma)<sub>2</sub>. Conversely, treatment of Ti(NMe<sub>2</sub>)<sub>4</sub> with 2 equiv of H<sub>2</sub>dpma does not provide Ti(dpma)<sub>2</sub>, which was available by addition of 2 Li<sub>2</sub>dpma to TiCl<sub>4</sub>. The properties of the isostructural series M(dpma)<sub>2</sub> were investigated by single crystal X-ray diffraction, cyclic voltammetry, <sup>14</sup>N NMR, and other techniques. By <sup>14</sup>N NMR, it was found that the pyrrolyl resonance chemical shift changes approximately linearly with the electronegativity of the metal center, which was attributed to  $\pi$ -interaction between the pyrrolyl nitrogen lone pair and the metal. Other complexes produced during this study include Ti(CH<sub>2</sub>SiMe<sub>3</sub>)(NMe<sub>2</sub>)(dpma), TiCl<sub>2</sub>(THF)(dpma), and Ti(OCH<sub>2</sub>CF<sub>3</sub>)<sub>2</sub>(THF)(dpma). Two isomers for Ti(CH<sub>2</sub>SiMe<sub>3</sub>)(NMe<sub>2</sub>)(dpma) were isolated and characterized.

### Introduction

Transition metal-amido<sup>1</sup>  $\pi$ -bond enthalpies are often accessible by dynamic NMR through measured barriers to rotation around the metal–nitrogen bond.<sup>2</sup> The barrier to rotation can vary from  $\sim 0$  to  $>23$  kcal/mol depending on the metal's Lewis acidity, orbital overlap considerations, and so forth. Commonly, early transition metal complexes in their highest oxidation state are stabilized by this substantial electron-donation from the amido group.

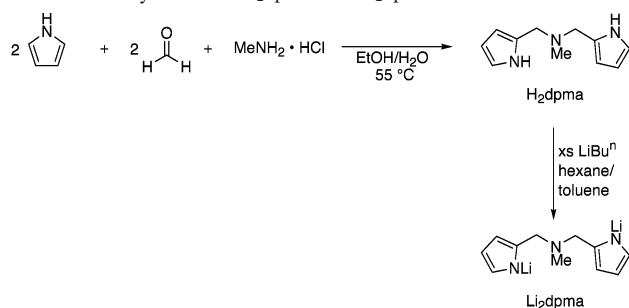
To increase the reactivity of amido complexes, attenuation of  $\pi$ -donation is often desirable. Several amido ligands from the ubiquitous hexamethyldisilazide<sup>1a</sup> to borylamides<sup>3</sup> have been utilized for this purpose. However, a different strategy involving  $\eta^1$ -pyrrolyl-based ligands has been less explored

for early transition metals.<sup>4</sup> Pyrrole has an aromatic stabilization energy (ASE) of  $\sim 24$  kcal/mol, cf. the ASE of benzene at  $\sim 35$  kcal/mol.<sup>5</sup> In addition, the aromatic  $\pi$ -system of pyrrole requires delocalization of the nitrogen lone pair in order to reach the 6  $\pi$ -electrons required by the Hückel rule. Consequently,  $\pi$ -donation from an  $\eta^1$ -pyrrolyl substituent to a pendant transition metal requires overcoming the substantial pyrrolyl ASE. Because the ASE of pyrrole and amido  $\pi$ -interaction may be of comparable energy with some metal centers, consideration of both  $\pi$ -donating and aromatic resonance forms is necessary.

\* To whom correspondence should be addressed. E-mail: odom@cem.msu.edu.

- (1) Transition metal-amido reviews: (a) Cummins, C. C. *Prog. Inorg. Chem.* **1998**, *47*, 685–835. (b) Kempe, R. *Angew. Chem., Int. Ed.* **2000**, *39*, 468–493. (c) Bryndza, H. E.; Tam, W. *Chem. Rev.* **1988**, *88*, 1163–1188. (d) Lappert, M. F.; Power, P. P.; Sanger, A. R.; Srivastava, R. C. *Metal and Metalloid Amides*; John Wiley & Sons: New York, 1980. (e) Gade, L. H. *Chem. Commun.* **2000**, 173–181.
- (2) (a) Chisholm, M. H.; Folting, K.; Huffman, J. C.; Rothwell, I. P. *Organometallics* **1982**, *1*, 251–259. (b) Odom, A. L.; Cummins, C. C. *Polyhedron* **1998**, *5–6*, 675–688.
- (3) (a) Warren, T. H.; Schrock, R. R.; Davis, W. M. *Organometallics* **1996**, *15*, 562–569. (b) Chen, H.; Bartlett, R. A.; Olmstead, M. M.; Power, P. P.; Shoner, S. C. *J. Am. Chem. Soc.* **1990**, *112*, 1048–1055.

- (4) Because of the different electronic structure due to the extended  $\pi$ -system, we exclude porphyrin and its many derivatives from the term pyrrolyl. Related porphyrinogen ligands should be included in this category. Examples of group-4 porphyrinogen complexes: (a) Bonomo, L.; Toraman, G.; Solari, E.; Scopelliti, R.; Floriani, C. *Organometallics* **1999**, *18*, 5198–5200. (b) Benech, J. M.; Bonomo, L.; Solari, E.; Scopelliti, R.; Floriani, C. *Angew. Chem., Int. Ed.* **1999**, *38*, 1957–1959. (c) Crescenzi, R.; Solari, E.; Floriani, C.; Re, N.; Chiesi-Villa, A.; Rizzoli, C. *Organometallics* **1999**, *18*, 606–618. (d) Floriani, C.; Solari, E.; Solari, G.; Chiesi-Villa, A.; Rizzoli, C. *Angew. Chem., Int. Ed.* **1998**, *37*, 2245–2248. (e) Solari, G.; Solari, E.; Lemercier, G.; Floriani, C.; Chiesi-Villa, A.; Rizzoli, C. *Inorg. Chem.* **1997**, *12*, 2691–2695. (f) Solari, G.; Solari, E.; Floriani, C.; Chiesi-Villa, A.; Rizzoli, C. *Organometallics* **1997**, *16*, 508–510. (g) Crescenzi, R.; Solari, E.; Floriani, C.; Chiesi-Villa, A.; Rizzoli, C. *Organometallics* **1996**, *15*, 5456–5458. (h) Solari, E.; Crescenzi, R.; Jacoby, D.; Floriani, C.; Chiesi-Villa, A.; Rizzoli, C. *Organometallics* **1996**, *15*, 2685–2687.
- (5) March, J. *Advanced Organic Chemistry*, 4th ed; John Wiley and Sons: New York, 1992.

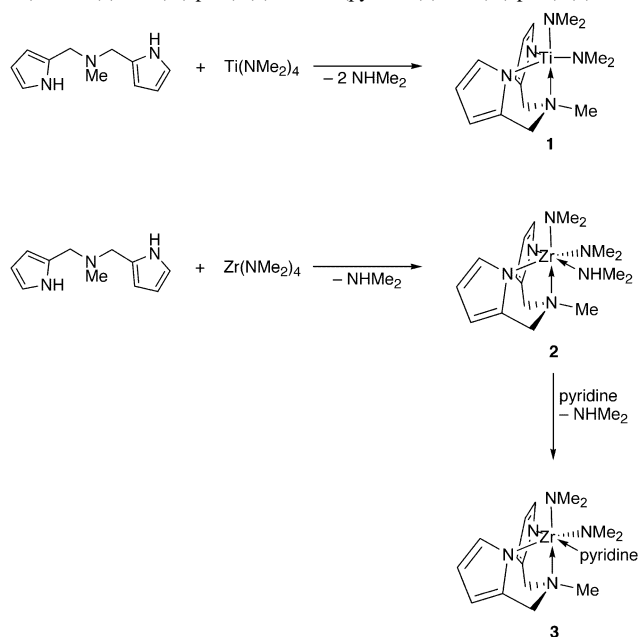
**Scheme 1.** Synthesis of  $H_2dpma$  and  $Li_2dpma$ 

In this report, we outline some chemistry of group-4 pyrrolyl complexes bearing dianionic, tridentate ligands. The study details synthetic protocols for complexes employed in studies on reactivity, metal-pyrrolyl bonding, and factors influencing fluxionality in these  $d^0$  complexes.

Some of the results included have been previously communicated.<sup>6</sup>

## Results and Discussion

The area of group-4 pyrrolyl complexes has been developing rapidly with a host of new ligands and complexes now reported.<sup>7</sup> Our group has focused on a particular pyrrolyl ligand framework, which is readily accessed by Mannich reactions involving amines and pyrrole. The simplest ligand of this class is prepared by reaction of 2 equiv of pyrrole, 2 equiv of formaldehyde, and 1 equiv of methylamine hydrochloride. The product is *N,N*-di(pyrrolyl- $\alpha$ -methyl)-*N*-methylamine or  $H_2dpma$  (Scheme 1). A literature preparation for  $H_2dpma$  has appeared.<sup>8</sup> In our hands, however, the literature procedure yields somewhat inconsistent results, and we have developed a slight modification that gives 60–80% yield of  $H_2dpma$  ( $\sim 15$  g scale) on a consistent basis. The lithium salt  $Li_2dpma$  is readily prepared in near quantitative yield as a solvent-free, colorless solid by treatment of  $H_2dpma$  in toluene with an excess of *n*-butyllithium in hexanes.

**Scheme 2.** Syntheses of  $Ti(NMe_2)_2(dpma)$  (**1**),  $Zr(NHMe_2)(NMe_2)_2(dpma)$  (**2**), and  $Zr(pyridine)(NMe_2)_2(dpma)$  (**3**)

The ligand preparation has proved quite flexible, and many derivatives of  $H_2dpma$  are accessible by utilizing substituted pyrroles, aldehydes in place of formaldehyde, and other alkylamines.<sup>9</sup> Difficulties in the syntheses only arise when the amine becomes quite bulky, which may cause the Mannich reaction to be prohibitively slow.

**Synthesis and Properties of Group-4  $dpma$  Bis(dimethylamide) Complexes.** Treatment of a  $Ti(NMe_2)_4$  solution with  $H_2dpma$  (Scheme 2) leads to near quantitative transamination generating  $Ti(NMe_2)_2(dpma)$  (**1**). The compound is readily isolated as a canary yellow solid after recrystallization but is sufficiently pure on generation for further use. Complex **1** is an active catalyst for the hydroamination of alkynes by primary amines.<sup>10</sup>

$Ti(NMe_2)_2(dpma)$  (**1**) has a trigonal bipyramidal structure in the solid state with one dimethylamido substituent axial and the other equatorial.<sup>6</sup> The 5-coordinate complex **1** does not rapidly exchange axial and equatorial substituents, and the two dimethylamido groups are inequivalent on the NMR time scale in fluid solution even at 80 °C.<sup>11</sup> NOE NMR experiments are consistent with the solid-state structure being retained in solution, and the spectrum was assigned using a combination of NOE and two-dimensional NMR spectroscopy. The protons of the equatorial dimethylamide group are  $\sim 0.2$  ppm more shielded than those in the axial amide group. In addition, the methylene protons *syn* to the *dpma* methyl are significantly more shielded than the *anti*-hydrogens.

Treatment of  $Zr(NMe_2)_4$  with  $H_2dpma$  results in 6-coordinate  $Zr(NHMe_2)(NMe_2)_2(dpma)$  (**2**) (Figure 1, Table 1).

(9) Ciszewski, J. T.; Cao, C.; Odom, A. L. Unpublished results.

(10) Cao, C.; Ciszewski, J. T.; Odom, A. L. *Organometallics* **2001**, *20*, 5011–5013.

(11) Similar effects have been seen with other dianionic, tridentate ligands. Schrock, R. R.; Seidel, S. W.; Schrod, Y.; Davis, W. M. *Organometallics* **1999**, *18*, 428–437.

(6) Harris, S. A.; Ciszewski, J. T.; Odom, A. L. *Inorg. Chem.* **2001**, *40*, 1987–1988.

(7) For group-4  $\eta^1$ -pyrrolyl complexes: (a) Rogers, R. D.; Bynum, R. V.; Atwood, J. L. *J. Crystallogr. Spectrosc. Res.* **1984**, *14*, 21. (b) Atwood, J. L.; Rogers, R. D.; Bynum, R. V. *Acta Crystallogr., Sect. C* **1984**, *40*, 1812. (c) Bynum, R. V.; Zhang, H.-M.; Hunter, W. E.; Atwood, J. L. *Can. J. Chem.* **1986**, *64*, 1304. (d) Lee, H.; Bonanno, J. B.; Hascall, T.; Cordaro, J.; Hahn, J. M.; Parkin, G. *J. Chem. Soc., Dalton Trans.* **1999**, 1365–1368. (e) Dias, A. R.; Galvao, A. M.; Galvao, A. C. *Collect. Czech. Chem. Commun.* **1998**, *63*, 182–186. (f) Riley, P. N.; Fanwick, P. E.; Rothwell, I. P. *J. Chem. Soc., Chem. Commun.* **1997**, 1109–1110. (g) Dreves, H.; Schmeisser, A.; Hartung, J.; Baumeister, U. *Chem. Ber.* **1996**, *129*, 853–857. (h) Knizhnikov, V. A.; Ol'dekop, Y. A. *Ser. Khim. Navuk* **1986**, 119–121. (i) Chalkoun, R.; Gervais, D. *Synth. React. Inorg. Met.-Org. Chem.* **1978**, *8*, 137–147. (j) Buerger, H.; Daemmgen, U. *Z. Anorg. Allg. Chem.* **1972**, *394*, 209–216. (k) Bradley, D. C.; Chivers, K. J. *J. Chem. Soc. A* **1968**, 1967–1969. (l) Yoshida, Y.; Matsui, S.; Takagi, Y.; Mitani, M.; Nitabaru, M.; Nakano, T.; Tanaka, H.; Fujita, T. *Chem. Lett.* **2000**, 1270. (m) Huang, J.-H.; Kuo, P.-C.; Lee, G.-H.; Peng, S.-M. *J. Chin. Chem. Soc.* **2000**, *47*, 1191. (n) Huang, J.-H.; Chi, L.-S.; Huang, F.-M.; Kuo, P.-C.; Zhou, C.-C.; Lee, G.-H.; Peng, S.-M. *J. Chin. Chem. Soc.* **2000**, *47*, 895–900. (o) Yoshida, Y.; Matsui, S.; Takagi, Y.; Mitani, M.; Nakano, T.; Tanaka, H.; Kashiwa, N.; Fujita, T. *Organometallics* **2001**, *20*, 4793–4799. For related group-4 carbazole chemistry see: Riley, P. N.; Fanwick, P. E.; Rothwell, I. P. *J. Chem. Soc., Dalton Trans.* **2001**, 181–186.

(8) Raines, S.; Kovacs, C. A. *J. Heterocycl. Chem.* **1970**, *7*, 223–225.

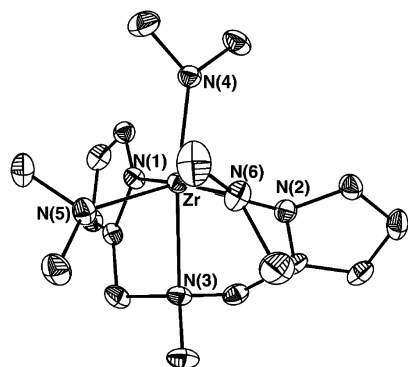
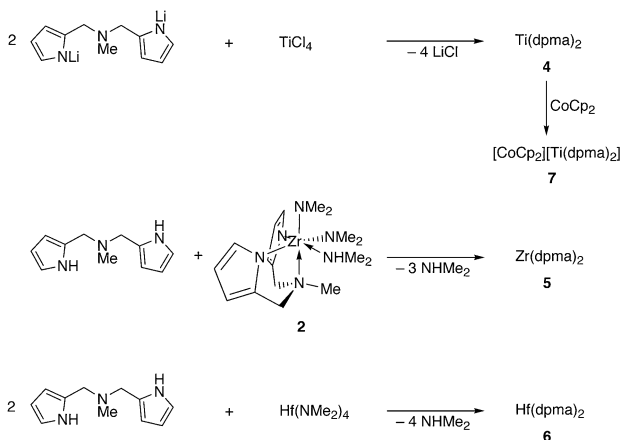


**Figure 1.** ORTEP diagram of  $\text{Zr}(\text{NMe}_2)_2(\text{NHMe}_2)(\text{dpma})$  (**2**) from single crystal X-ray diffraction.

**Table 1.** Selected Bond Distances (Å) and Angles (deg) from the X-ray Diffraction Study on  $\text{Zr}(\text{NMe}_2)_2(\text{NHMe}_2)(\text{dpma})$  (**2**)

|              |            |              |            |
|--------------|------------|--------------|------------|
| Zr–N(5)      | 2.038(4)   | Zr–N(4)      | 2.047(4)   |
| Zr–N(4)      | 2.047(4)   | Zr–N(1)      | 2.222(4)   |
| Zr–N(2)      | 2.242(4)   | Zr–N(6)      | 2.462(4)   |
| Zr–N(3)      | 2.490(3)   |              |            |
|              |            |              |            |
| N(5)–Zr–N(4) | 109.57(15) | N(5)–Zr–N(4) | 109.57(15) |
| N(5)–Zr–N(1) | 96.57(16)  | N(4)–Zr–N(1) | 91.91(13)  |
| N(5)–Zr–N(2) | 146.68(14) | N(4)–Zr–N(2) | 98.12(14)  |
| N(1)–Zr–N(2) | 100.77(14) | N(5)–Zr–N(6) | 84.73(14)  |
| N(4)–Zr–N(6) | 90.62(14)  | N(1)–Zr–N(6) | 176.59(13) |
| N(2)–Zr–N(6) | 76.60(13)  | N(5)–Zr–N(3) | 88.95(14)  |
| N(4)–Zr–N(3) | 155.94(15) | N(1)–Zr–N(3) | 70.19(12)  |
| N(2)–Zr–N(3) | 70.82(13)  | N(6)–Zr–N(3) | 106.73(12) |

**Scheme 3.** Syntheses of  $\text{M}(\text{dpma})_2$  Complexes 4–7



The complex is readily isolated and stable as the dimethylamine adduct. However, the dimethylamine is readily substituted by pyridine affording  $\text{Zr}(\text{pyridine})(\text{NMe}_2)_2(\text{dpma})$  (**3**).

Unlike in the structure of  $\text{Ti}(\text{NMe}_2)_2(\text{dpma})$  (**1**),<sup>6</sup> the equatorial dimethylamide does not have the amide N,C,C-plane perpendicular to the axial amide plane to avoid competition between these two  $\pi$ -donors. In the case of **2**,  $\pi$ -donation from the amides may be of less energetic importance relative to **1** because of the added donor and electronic differences between titanium and zirconium, e.g. bond polarity.

**Group 4 Bis(dpma) Complexes.** Reactions were carried out between 1 equiv of  $\text{Li}_2\text{dpma}$  and  $\text{TiCl}_4$  (Scheme 3). With

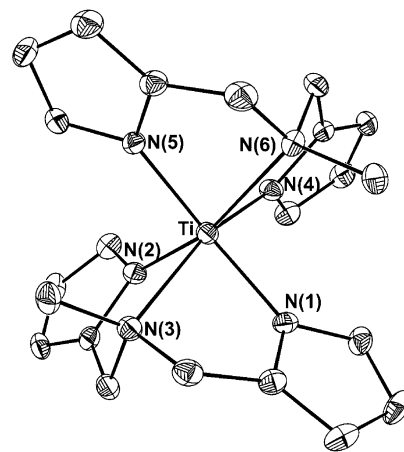


**Figure 2.** ORTEP representation of the structure of  $\text{Ti}(\text{dpma})_2$  (**4**) found by X-ray diffraction.

1, 2, 4, or 8 equiv of  $\text{TiCl}_4$ , we observe a single isolable product,  $\text{Ti}(\text{dpma})_2$  (**4**). Hexacoordinate **4** has a brick red color in solution and is somewhat moisture sensitive.

In addition to salt elimination routes, we have explored other dimethylamido replacement strategies. As mentioned, treating  $\text{Ti}(\text{NMe}_2)_4$  with  $\text{H}_2\text{dpma}$  results in clean formation of  $\text{Ti}(\text{NMe}_2)_2(\text{dpma})$  (**1**). Reactions involving  $\text{Ti}(\text{NMe}_2)_4$  and multiple equivalents of  $\text{H}_2\text{dpma}$  have not yielded **4**, and **1** is the only isolated product. The cause for the lack of reactivity between  $\text{Ti}(\text{NMe}_2)_2(\text{dpma})$  and  $\text{H}_2\text{dpma}$  is found in the electronics of **1**. Bis(dimethylamido) **1** has quite short Ti–N(dimethylamido) bonds consistent with significant Ti–N multiple bonding.<sup>6</sup> Substantial donation from the dimethylamido lone pairs results in slow reactions with many protic reagents.

In the solid state,  $\text{Ti}(\text{dpma})_2$  (**4**) exhibits approximate  $C_2$  symmetry (Figure 2). The flexible tridentate ligands acquire a *fac*-coordination geometry with the donor nitrogen of one dpma *trans* to a pyrrolyl substituent of the cohabitant dpma. The Ti–N(donor) distances were found to average 2.308(3) Å. The Ti–N(pyrrolyl) distances averaged 1.989(3) Å. All of the Ti–N(pyrrolyl) distances were the same within statistical variation, and no *trans*-influences are evident. Several large discrepancies from octahedral angles are observed in the solid-state structure. The angular deviations from an octahedral primary coordination environment are attributable to restrictions due to chelation. The  $C_2$  symmetry of **4** in the solid state appears to be retained in solution by <sup>1</sup>H and <sup>13</sup>C NMR spectroscopy.

In contrast to the titanium system,  $\text{Zr}(\text{NMe}_2)_4$  and  $\text{Hf}(\text{NMe}_2)_4$  do react with multiple equivalents of  $\text{H}_2\text{dpma}$  to give bis(dpma) complexes  $\text{Zr}(\text{dpma})_2$  (**5**) and  $\text{Hf}(\text{dpma})_2$  (**6**). However, **5** is most cleanly prepared by treating purified  $\text{Zr}(\text{NMe}_2)_2(\text{NHMe}_2)(\text{dpma})$  (**2**) with  $\text{H}_2\text{dpma}$ . Thus far, we have not been successful in substituting only 2 dimethylamides on  $\text{Hf}(\text{NMe}_2)_4$  with  $\text{H}_2\text{dpma}$  by transamination to give  $\text{Hf}(\text{NMe}_2)_2(\text{NHMe}_2)(\text{dpma})$ , and all attempts have resulted in **6**.

The solid-state structures of **5** and **6** are analogous to that of titanium derivative **4** with approximate  $C_2$  symmetry. Some pertinent structural data are collected in Table 2.

**Table 2.** Structural Parameters for  $M(\text{dpma})_2$  from Single Crystal X-ray Diffraction, Where  $M = \text{Ti(IV)}$  (2),  $\text{Zr(IV)}$  (5),  $\text{Hf(IV)}$  (6), and  $\text{Ti(III)}$  (7)

|  | Ti(IV) (4)                                      | Zr(IV) (5)  | Hf(IV) (6)  | Ti(III) (7)                                       |
|--|---|---|---|---|
| formula                                  | $\text{C}_{22}\text{H}_{26}\text{N}_6\text{Ti}$ | $\text{C}_{22}\text{H}_{26}\text{N}_6\text{Zr}^+\text{C}_6\text{H}_6$ | $\text{C}_{22}\text{H}_{26}\text{N}_6\text{Hf}^+\text{CH}_2\text{Cl}_2$ | $\text{C}_{32}\text{H}_{36}\text{CoN}_6\text{Ti}$ |
| fw                                       | 422.39  | 543.82  | 637.90  | 611.50  |
| space group                              | $P2_1/n$  | $Cc$  | $P2_1/n$  | $P2_1/c$  |
| $a$ (Å)                                  | 10.470(2)                                       | 8.7315(12)  | 8.47(2)   | 17.692  |
| $b$ (Å)                                  | 17.479(4)                                       | 15.993(2)   | 17.56(5)  | 29.628  |
| $c$ (Å)                                  | 11.766(2)                                       | 18.719(3)   | 15.95(4)  | 11.272(7)   |
| $\beta$ (deg)                            | 102.13(3)                                       | 96.471(2)   | 93.97(5)  | 100.80(4)   |
| $V$ (Å <sup>3</sup> )                    | 2105.2(7)                                       | 2597.3(6)   | 2368(11)  | 5804(5)   |
| $Z$                                      | 4   | 4   | 4   | 8   |
| $\mu$ (mm <sup>-1</sup> )                | 0.427   | 0.451   | 4.655   | 0.879   |
| $D_{\text{calcd}}$ (g cm <sup>-3</sup> ) | 1.333   | 1.391   | 1.789   | 1.400   |
| $R(F_o)$ ( $I > 2\sigma$ )               | 0.0429  | 0.0366  | 0.0529  | 0.0620  |
| $R_w(F_o^2)$ ( $I > 2\sigma$ )           | 0.0817  | 0.0853  | 0.1520  | 0.1170  |
| $M-N_{\text{pyrrolyl}}$ (Å)              | 1.989(3)  | 2.135(9)  | 2.113(9)  | 2.079(6)  |
| $M-N_{\text{amine}}$ (Å)                 | 2.308(3)  | 2.44(1)   | 2.40(1)   | 2.342(6)  |
| $N(5)-M-N(1)$ (deg)                      | 146.4(1)  | 134.3(2)  | 140.7(3)  | 153.0(2)  |
| $N(6)-M-N(2)$ (deg)                      | 162.4(1)  | 155.1(3)  | 157.5(3)  | 166.7(2)  |
| $N(4)-M-N(3)$ (deg)                      | 161.3(1)  | 154.2(3)  | 157.8(3)  | 164.1(2)  |

Like many hexacoordinate metal complexes<sup>12</sup> with heterocyclic ligands,<sup>13</sup>  $\text{Ti}(\text{dpma})_2$  exhibits reversible redox behavior.<sup>14</sup> The cyclic voltammogram referenced to the  $\text{FeCp}_2^{0/+}$  couple was carried out in chlorobenzene with tetrabutylammonium triflate as the electrolyte. The  $\text{Ti}(\text{dpma})_2^{-1/0}$  redox couple was found at  $-1.26$  V. Chemically, the reduction can be carried out with  $\text{CoCp}_2$ . Solutions of  $\text{Ti}(\text{dpma})_2$  treated with cobaltocene (Scheme 3) yield  $[\text{CoCp}_2]\text{-}[\text{Ti}(\text{dpma})_2]$  (7) as a brown solid.

Single crystal X-ray diffraction on 7 reveals separate  $[\text{Ti}(\text{dpma})_2]^-$  and  $[\text{CoCp}_2]^+$  ions with no close contacts. The complex crystallized with two chemically equivalent molecules in the asymmetric unit. The titanium anion is structurally similar to 4 with expected increases in  $\text{Ti-N}$  bond distances on reduction to titanium(III).

Cyclic voltammetry on  $\text{Zr}(\text{dpma})_2$  (5) and  $\text{Hf}(\text{dpma})_2$  (6) afforded irreversible reductions with half-wave potentials at  $-1.405$  and  $-1.565$  V, respectively.

**<sup>14</sup>N NMR on  $M(\text{dpma})_2$  Complexes.** Nitrogen NMR<sup>15</sup> has been used to evaluate the  $\pi$ -electron density of azoles.<sup>16</sup> The chemical shift has been found to correlate with calculated

$\pi$ -charge densities (SCF-PPP-MO method) of the aromatic ring. Considering the aromaticity of pyrrole is dependent upon the delocalization of the nitrogen lone pair, competition between the aromatic system and metal-based orbitals for the lone pair should attenuate the  $\pi$ -electron density. Therefore, a link between nitrogen NMR chemical shifts and  $\pi$ -acceptor ability of the metal center might be expected. Consistent with this,  $N$ -substituted pyrrolyl compounds where the substituents are methyl groups versus boranes and silanes vary over a range of about 30 ppm.<sup>17</sup> In addition, greater  $M-N(\text{pyrrolyl})$  bond polarity may affect nitrogen  $\sigma \rightarrow \pi^*$  excitation and alter the <sup>14</sup>N NMR chemical shift.<sup>18</sup>

Chemical shifts of coordinated amines may also be affected by the metal center.<sup>15</sup> For closed-shell metal centers, such as the  $d^0$  complexes in this study, the resonance typically shifts downfield relative to the free amine.

The <sup>14</sup>N NMR chemical shift of pyrrole is  $-235$  ppm relative to neat nitromethane.<sup>17</sup> Examination of  $\text{H}_2\text{dpma}$  resulted in a single resonance for the compound at  $-234$  ppm, which is assigned to the pyrrolyl nitrogens. It is currently unknown whether the amine nitrogen is coincident with the pyrrolyl resonance or is too broad to locate.

For the complexes  $M^{\text{IV}}(\text{dpma})_2$  (4–6), where  $M$  is Ti, Zr, and Hf, the pyrrolyl nitrogen <sup>14</sup>N NMR chemical shifts are  $-84$ ,  $-128$ , and  $-131$  ppm, respectively. The resonances shift significantly on coordination from the chemical shift in  $\text{H}_2\text{dpma}$ . The electronegativities of titanium, zirconium, and hafnium in the +4 oxidation state are approximately 1.50, 0.90, and 0.81 on the Pauling scale, respectively.<sup>19</sup> Interestingly, the pyrrolyl chemical shifts vary almost linearly with the electronegativities of the three metals in the +4 oxidation state, as shown in Figure 3.<sup>20</sup> Because  $\sigma$ -bond polarity and nitrogen lone pair donation to the metal could potentially perturb the chemical shift, it is difficult to determine if the shifts are due to  $\sigma$ -effects,  $\pi$ -effects, or a combination of the two. However, we have prepared a series of group-6 imido complexes where any  $\pi$ -bonding from the pyrrolyl substituents must compete with the strong  $\pi$ -bonds of imido substituents.<sup>21</sup> Pyrrolyl chemical shifts for this series change relatively little on proceeding through the triad. Consequently, the data for  $M(\text{dpma})_2$  and other *dpma*

- (12) For some leading general references on transition metals with nitrogen heterocyclic ligands see: (a) Braterman, P. S.; Song, J.-I.; Peacock, R. D. *Inorg. Chem.* **1992**, *31*, 555–559. (b) Reger, D. L.; Little, C. A.; Rheingold, A. L.; Lam, M.; Concolino, T.; Mohan, A.; Long, G. *J. Inorg. Chem.* **2000**, *39*, 4674–5. (c) Trofimenko, S. *Prog. Inorg. Chem.* **1986**, *34*, 115–210. (d) Trofimenko, S. *Chem. Rev.* **1993**, *93*, 943–980. (e) Etienne, M. *Coord. Chem. Rev.* **1996**, *156*, 201–236.
- (13) Some leading references on  $M(\text{bpy})_3$  group-4 complexes: (a) Beckhaus, R.; Thiele, K.-H. *J. Organomet. Chem.* **1986**, *317*, 23–31. (b) Quirk, J.; Wilkinson, G. *Polyhedron* **1982**, *1*, 209–211. (c) Rosa, P.; Mézailles, N.; Ricard, L.; Mathey, F.; Le Floch, P. *Angew. Chem., Int. Ed.* **2000**, *39*, 1823–1926.
- (14) Within group-4 complexes, the reactive titanium(II) complex  $\text{TiTp}_2$  was recently reported: (a) Kayal, A.; Kuncheria, J.; Lee, S. C. *Chem. Commun.* **2001**, 2482–2483. (b) For a related report on  $\text{V}(\text{Tp})_2$ : Dapporto, P.; Mani, F.; Mealli, C. *Inorg. Chem.* **1978**, *17*, 1323–1329.
- (15) (a) Mason, J. *Chem. Rev.* **1981**, *81*, 205–227. (b) Mason, J. In *Multinuclear NMR*; Mason, J., Ed.; Nitrogen; Plenum: New York, 1987.
- (16) Witanowski, M.; Stefaniak, L.; Januszewski, H.; Grabowski, Z. *Tetrahedron* **1972**, *28*, 637–653.

- (17) Chadwick, D. J. *Physical and Theoretical Aspects of 1H-Pyrroles*. In *Pyrroles*, Part I; Jones, A. R., Ed.; The Chemistry of Heterocyclic Compounds; John Wiley & Sons: New York, 1990.
- (18) This type of effect can be seen in the nitrogen NMR of pyridine and pyridinium. See reference 15 for a complete discussion.
- (19) For a discussion of electronegativity and formal oxidation states: (a) Sanderson, R. T. *Inorg. Chem.* **1986**, *25*, 3518. (b) Sanderson, R. T. *J. Chem. Educ.* **1988**, *65*, 112–118; 227–231. (c) Sanderson, R. T. *Polar Covalence*; Academic Press: New York, 1983.
- (20) Linear correlations of electronegativity and NMR shifts are well-known, for organic compounds in particular. The relation is often valid for compounds with similar structural and electronic considerations, such as the  $M(\text{dpma})_2$  complexes presented. For some seminal papers see: (a) Spiesscke, H.; Schneider, W. G. *J. Chem. Phys.* **1961**, *35*, 722–730. (b) Cavanaugh, J. R.; Dailey, B. P. *J. Chem. Phys.* **1961**, *34*, 1099–1107.
- (21) We have prepared the series  $M(\text{NBu})_2(\text{dpma})$  where  $M = \text{Cr, Mo, and W}$ . The resonances for the pyrrolyl nitrogens only vary over a 6 ppm range in contrast to the  $\sim 50$  ppm range for the bis(*dpma*) complexes discussed in this study. Ciszewski, J. T.; Odom, A. L. Manuscript in preparation.

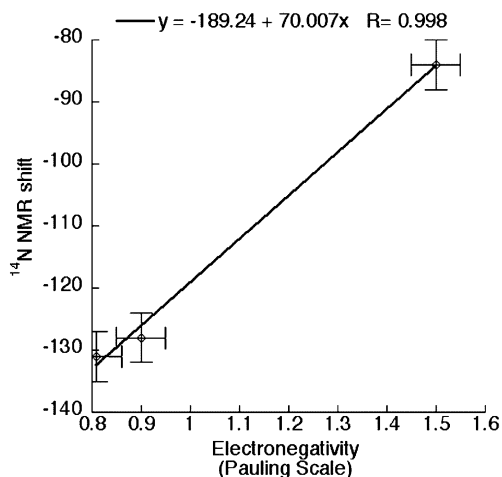
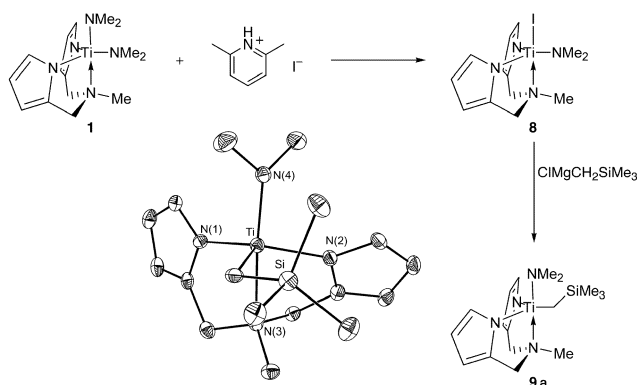


**Figure 3.** Plot of pyrrolyl  $^{14}\text{N}$  NMR chemical shift versus metal electronegativity for  $\text{M}(\text{dpma})_2$  complexes. Error bars are for 0.05 in electronegativity, which is approximately that suggested by Sanderson for the metal centers in the oxidation state of interest.<sup>19</sup> An error of 5 ppm was used for these relatively broad  $^{14}\text{N}$  NMR resonances.

**Scheme 4.** Synthesis of  $\text{Ti}(\text{I})(\text{NMe}_2)(\text{dpma})$  (**8**) and  $\text{Ti}(\text{CH}_2\text{SiMe}_3)(\text{NMe}_2)(\text{dpma})$  (**9a**) with the ORTEP Diagram of the Solid-State Structure of **9a**



complexes are consistent with  $^{14}\text{N}$  NMR chemical shifts largely being sensitive to the  $\pi$ -acceptor ability of the metal center.

In contrast to the pyrrolyl  $^{14}\text{N}$  NMR chemical shifts, the amine resonances do not change significantly through the  $\text{M}(\text{dpma})_2$  series. The amine shifts for complexes **4–6** were found to be  $-238 \pm 1$  ppm.

**Group-4 dpma Halide and Alkoxide Complexes.** Treatment of  $\text{TiCl}_4$  with  $\text{Li}_2\text{dpma}$  does not afford  $\text{TiCl}_2(\text{dpma})$  as the major product (vide supra). Consequently, we sought an alternative route to titanium halide dpma complexes. Protolytic replacement of dimethylamides on  $\text{Ti}(\text{NMe}_2)_2(\text{dpma})$  (**1**) was investigated with 2,6-lutidinium iodide,<sup>22</sup> yielding the monoiodide  $\text{Ti}(\text{I})(\text{NMe}_2)(\text{dpma})$  (**8**).<sup>6</sup> Reaction with excess 2,6-lutidinium iodide did not lead to further dimethylamide replacement.

As shown in Scheme 4, the organometallic complex  $\text{Ti}(\text{equatorial-CH}_2\text{SiMe}_3)(\text{axial-NMe}_2)(\text{dpma})$  (**9a**) is accessible by metathesis on **8** with  $\text{ClMgCH}_2\text{SiMe}_3$  in dioxane/DME. The complex displays a pseudo-trigonal-bipyramidal geom-

**Table 3.** Selected Bond Distances ( $\text{\AA}$ ) and Angles (deg) from the X-ray Diffraction Study on  $\text{Ti}(\text{CH}_2\text{SiMe}_3)(\text{NMe}_2)(\text{dpma})$  (**9a**)

|              |            |              |            |
|--------------|------------|--------------|------------|
| Ti–N(4)      | 1.878(3)   | Ti–N(2)      | 2.002(3)   |
| Ti–N(1)      | 2.008(3)   | Ti–C(1)      | 2.081(4)   |
| Ti–N(3)      | 2.353(3)   |              |            |
| N(4)–Ti–N(2) | 97.38(14)  | N(4)–Ti–N(1) | 96.86(13)  |
| N(2)–Ti–N(1) | 125.39(13) | N(4)–Ti–C(1) | 102.37(15) |
| N(2)–Ti–C(1) | 114.78(15) | N(1)–Ti–C(1) | 112.98(14) |
| N(4)–Ti–N(3) | 162.54(12) | N(2)–Ti–N(3) | 75.60(12)  |
| N(1)–Ti–N(3) | 75.37(12)  | C(1)–Ti–N(3) | 95.07(13)  |

etry in the solid-state. The titanium–element distances overall are unremarkable in the context of other dpma complexes with a Ti–N(dimethylamide) distance, 1.878(3)  $\text{\AA}$  (Table 3), that is very similar to the Ti–N axial dimethylamide bond length in **1**.<sup>6</sup> A second isomer of  $\text{Ti}(\text{CH}_2\text{SiMe}_3)(\text{NMe}_2)(\text{dpma})$  has been isolated. Spectroscopic studies on the isomer identify it as  $\text{Ti}(\text{axial-CH}_2\text{SiMe}_3)(\text{equatorial-NMe}_2)(\text{dpma})$  (**9b**). In the crude reaction mixture, **9a** is formed with a slight preference over **9b** in a ratio of 1.8:1. Interconversion between isomers occurs at room temperature but is relatively slow. However, heating a solution of **9b** at 60  $^\circ\text{C}$  caused equilibration of the isomers, which is complete in less than an hour. Isomer **9a** is favored slightly with a  $K_{\text{eq}} = 1.2$  by  $^1\text{H}$  NMR.

Crystal structures of iodide **8** and alkyl **9** have the dpma ligand residing in a *fac*-position. The two monodentate substituents are axial and equatorial. The favored positions for the monodentate ligands in these complexes are consistent with expectations from a simple VSEPR model<sup>23</sup> with the larger substituent<sup>24</sup> residing in the equatorial position in both cases.

Black dichloro  $\text{TiCl}_2(\text{THF})(\text{dpma})$  (**10**) is accessible from **1** by reaction with  $\text{ClSiMe}_3$  in the presence of THF.<sup>25</sup> Titanium–N(pyrrolyl) distances in more electron-rich  $\text{Ti}(\text{NMe}_2)_2(\text{dpma})$  (**1**) averaged 2.016(3)  $\text{\AA}$ , significantly longer than the 1.969(2)  $\text{\AA}$  distance of **10**. Considering higher coordinate **10** displays significantly shortened Ti–N(pyrrolyl) distances, it is reasonable to postulate greater electron-donation from the pyrrolyl substituents in more electron-deficient **10**. However, the effect may also be the result of  $\sigma$ -inductive effects and orbital contractions due to the more electronegative ligand set of **10**.

(23) For an excellent general discussion of VSEPR theory see: Huheey, J. E. *Inorganic Chemistry: Principles of Structure and Reactivity*, 2nd ed.; Harper & Row Publishers: New York, 1978; Chapter 5.

(24) Unfortunately, we were unsuccessful in finding a single study on steric effect quantification that incorporates iodide, dimethylamide, and trimethylsilylmethyl. However, looking at cone angles on phosphorus for  $\text{PX}_3$  where X is bromide, dimethylamide, and neopentyl establishes the increasing size through this series. (a) Tolman, C. A. *Chem. Rev.* **1977**, *77*, 313. The sizes of iodide/bromide and neopentyl/trimethylsilylmethyl are very similar, as might be expected. (b) White, D. P.; Anthony, J. C.; Oyefeso, A. O. *J. Org. Chem.* **1999**, *64*, 7707–7716. Alternatively, the series I, *iso*-propyl, and trimethylsilylmethyl may be examined with the assumption that  $\text{NMe}_2$  will be sterically similar to  $\text{CHMe}_2$ . Reference b using ligand repulsive energies places these ligands in the order I, *iso*-propyl, and trimethylsilylmethyl with values of 4.0, 45, and 52 kcal/mol, respectively.

(25) Reaction of  $\text{ClSiMe}_3$  with amides is a now common synthetic technique for amido to halide exchange. For example: (a) Schrock, R. R.; Baumann, R.; Reid, S. M.; Goodman, J. T.; Stumpf, R.; Davis, W. M. *Organometallics* **1999**, *18*, 3649–3670. (b) Arney, D. J.; Bruck, M. A.; Huber, S. R.; Wigley, D. E. *Inorg. Chem.* **1992**, *31*, 3749–3755.

(22) (a) Odom, A. L.; Cummins, C. C. *Organometallics* **1996**, *15*, 898. (b) Odom, A. L.; Cummins, C. C. *Polyhedron* **1998**, *5–6*, 675–688.

**Scheme 5.** Syntheses of  $\text{TiCl}_2(\text{THF})(\text{dpma})$  (**10**) and  $\text{Ti}(\text{OCH}_2\text{CF}_3)_2(\text{THF})(\text{dpma})$  (**11**) with the ORTEP Diagrams from Their Solid-State Structures.

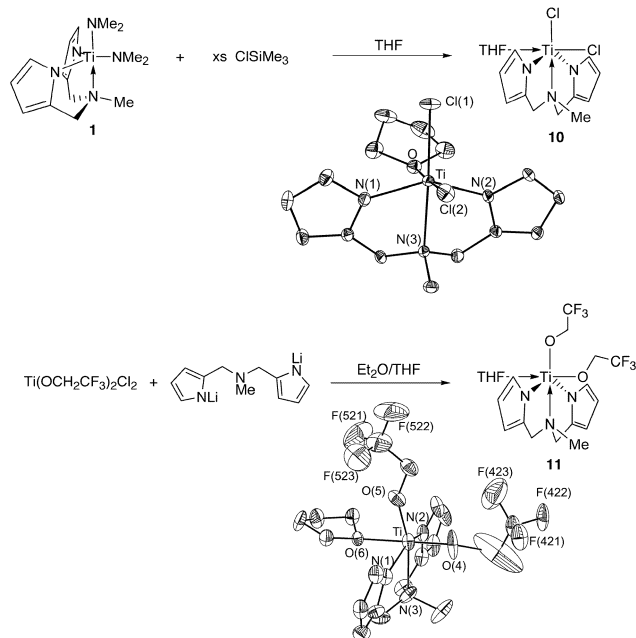


**Table 4.** Structural Parameters for  $\text{Zr}(\text{NMe}_2)_2(\text{NHMe}_2)(\text{dpma})$  (**2**),  $\text{Ti}(\text{CH}_2\text{SiMe}_3)(\text{NMe}_2)(\text{dpma})$  (**9**),  $\text{TiCl}_2(\text{THF})(\text{dpma})$  (**10**), and  $\text{Ti}(\text{OCH}_2\text{CF}_3)_2(\text{THF})(\text{dpma})$  (**11**) from Single Crystal X-ray Diffraction

|  | <b>2</b>  | <b>9</b>  | <b>10</b>  | <b>11</b>  |
|--|---|---|--|--|
| formula  | $\text{C}_{17}\text{H}_{31}\text{N}_6\text{Zr}$ | $\text{C}_{17}\text{H}_{30}\text{N}_4\text{SiTi}$ | $\text{C}_{15}\text{H}_{21}\text{Cl}_2\text{-N}_3\text{OTi}$ | $\text{C}_{19}\text{H}_{25}\text{F}_6\text{-N}_3\text{O}_3\text{Ti}$ |
| fw   | 410.70  | 366.44  | 378.15   | 505.32   |
| space group  | <i>R3c</i>                                      | <i>C2/c</i>                                       | <i>P2<sub>1</sub>/n</i>                                      | <i>Cc</i>  |
| <i>a</i> (Å)   | 26.127(2)                                       | 28.646(11)  | 9.032(3)   | 17.177   |
| <i>b</i> (Å)   | 26.127(2)                                       | 8.568(3)  | 16.671(4)  | 16.560(7)  |
| <i>c</i> (Å)   | 15.5158(19)                                     | 20.885(9)   | 11.624(4)  | 8.497(3)   |
| $\beta$ (deg)  | 90  | 129.70(3)   | 98.65(4)   | 108.18(3)  |
| <i>V</i> (Å <sup>3</sup> )                                   | 9172.7(16)                                      | 3944(3)   | 1730.4(10)   | 2296.2(19)   |
| <i>Z</i>   | 9   | 8   | 4  | 4  |
| $\mu$ (mm <sup>-1</sup> )                                    | 0.550   | 0.500   | 0.807  | 0.446  |
| <i>D</i> <sub>calcd</sub> (g cm <sup>-3</sup> )              | 1.338   | 1.234   | 1.451  | 1.462  |
| <i>R</i> ( <i>F</i> <sub>o</sub> )                           | 0.0257  | 0.0473  | 0.0282   | 0.0623   |
| <i>R</i> <sub>w</sub> ( <i>F</i> <sub>o</sub> <sup>2</sup> ) | 0.0688  | 0.1206  | 0.0717   | 0.1651   |

Alkoxides are often utilized in metathesis reactions for circumstances where the metal center is prone to reduction.<sup>26</sup> Consequently, synthetic routes to titanium *dpma* alkoxide complexes were explored as well. Bis(trifluoroethoxy)  $\text{Ti}(\text{OCH}_2\text{CF}_3)_2(\text{dpma})(\text{THF})$  (**11**) is accessible from  $\text{Ti}(\text{OCH}_2\text{CF}_3)_2\text{Cl}_2$ <sup>27</sup> and  $\text{Li}_2\text{dpma}$ . The solid-state structure of **11** is displayed in Scheme 5. Even though the model of the structure accounts for the electron density quite well,  $R(F_o) = 0.0623$  and  $R_w(F_o^2) = 0.1651$  (Table 4), large thermal motion resulted in a structure with relatively large esd's on structural parameters making quantitative comparisons less

(26) For examples of alkyl for alkoxide metathesis to lessen problems with metal center reduction see the syntheses of  $\text{CrMe}_4$ ,  $\text{NMoNp}_3$ , and  $\text{NCr}(\text{CH}_2\text{SiMe}_3)_2(\text{NPr}_2)$ : (a) Mowat, W.; Shortland, A. J.; Hill, N. J.; Wilkinson, G. *J. Chem. Soc., Dalton Trans.* **1973**, 770–8. (b) Herrmann, W. A.; Bogdanovic, S.; Poli, R.; Priermeier, T. *J. Am. Chem. Soc.* **1994**, *116*, 4989–90. (c) Odom, A. L.; Cummins, C. C. *Polyhedron* **1998**, *5–6*, 675–688.

(27) (a) Basso-Bert, M.; Gervais, D. *Inorg. Chim. Acta* **1979**, *34*, 191–5. (b) Paul, R. C.; Gupta, P. K.; Gulati, M.; Chadha, S. L. *Inorg. Nucl. Chem. Lett.* **1977**, *13*, 665–8.

**Table 5.** Selected Bond Distances (Å) and Angles (deg) from the X-ray Diffraction Study on  $\text{TiCl}_2(\text{THF})(\text{dpma})$  (**10**)

|               |            |                |            |
|---------------|------------|----------------|------------|
| Ti–N(1)       | 1.963(2)   | Ti–N(3)        | 2.3055(18) |
| Ti–O          | 2.1845(18) | Ti–N(2)        | 1.9740(19) |
| Ti–Cl(2)      | 2.2590(11) | Ti–Cl(1)       | 2.2745(9)  |
| N(1)–Ti–O     | 85.54(8)   | N(2)–Ti–O      | 85.94(8)   |
| N(2)–Ti–N(1)  | 147.09(7)  | N(1)–Ti–Cl(2)  | 95.32(7)   |
| N(2)–Ti–Cl(2) | 95.23(7)   | O–Ti–Cl(2)     | 176.25(5)  |
| N(1)–Ti–Cl(1) | 106.71(6)  | N(2)–Ti–Cl(1)  | 103.77(5)  |
| O–Ti–Cl(1)    | 83.35(4)   | Cl(2)–Ti–Cl(1) | 92.92(3)   |
| N(1)–Ti–N(3)  | 73.41(7)   | N(2)–Ti–N(3)   | 73.88(7)   |
| O–Ti–N(3)     | 80.95(6)   | Cl(2)–Ti–N(3)  | 102.79(5)  |
| Cl(1)–Ti–N(3) | 164.25(5)  |                |            |

**Table 6.** Selected Bond Distances (Å) and Angles (deg) from the X-ray Diffraction Study on  $\text{Ti}(\text{OCH}_2\text{CF}_3)_2(\text{THF})(\text{dpma})$  (**11**)

|              |          |              |          |
|--------------|----------|--------------|----------|
| Ti–N(1)      | 2.027(7) | Ti–N(3)      | 2.310(8) |
| Ti–O(4)      | 1.799(6) | Ti–N(2)      | 2.004(7) |
| Ti–O(5)      | 1.784(6) | Ti–O(6)      | 2.213(5) |
| O(5)–Ti–O(4) | 98.2(4)  | O(5)–Ti–N(2) | 104.2(3) |
| O(4)–Ti–N(2) | 94.5(3)  | O(5)–Ti–N(1) | 104.0(3) |
| O(4)–Ti–N(1) | 97.0(3)  | N(2)–Ti–N(1) | 147.7(3) |
| O(5)–Ti–O(6) | 83.2(3)  | O(4)–Ti–O(6) | 176.6(2) |
| N(2)–Ti–O(6) | 82.2(2)  | N(1)–Ti–O(6) | 85.6(2)  |
| O(5)–Ti–N(3) | 165.3(3) | O(4)–Ti–N(3) | 96.6(4)  |
| N(2)–Ti–N(3) | 74.8(3)  | N(1)–Ti–N(3) | 73.9(3)  |
| O(6)–Ti–N(3) | 82.1(2)  |              |          |

fruitful. However, the apparent bond distances are similar to those of dichloro **10** (Tables 5 and 6).

## Concluding Remarks

This investigation into group-4 pyrrolyl chemistry has focused on the chelating ligand *dpma*, which is readily prepared in high yield from inexpensive starting materials. Transamination of dimethylamides on  $\text{Ti}(\text{NMe}_2)_4$  and  $\text{Zr}(\text{NMe}_2)_4$  with  $\text{H}_2\text{dpma}$  results in clean protonation of 2 dimethylamides to form  $\text{Ti}(\text{NMe}_2)_2(\text{dpma})$  (**1**) and  $\text{Zr}(\text{NMe}_2)_2(\text{NHMe}_2)(\text{dpma})$  (**2**), respectively.

Examinations regarding reactivity and properties within this system have been consistent with some anticipated differences between amido-metal bonds where the metal is systematically altered from the 1st to the 3rd row of group-4. The reactivity of  $\text{M}(\text{NMe}_2)_2(\text{dpma})$  with  $\text{H}_2\text{dpma}$  dramatically demonstrates the difference in amido basicity as one proceeds down the column. Relatively strong Ti–N  $\pi$ -bonding in **1** and low bond polarity results in no reaction between  $\text{Ti}(\text{NMe}_2)_2(\text{dpma})$  and  $\text{H}_2\text{dpma}$ . Conversely,  $\text{Zr}(\text{NMe}_2)_2(\text{NHMe}_2)(\text{dpma})$  (**2**) reacts cleanly with  $\text{H}_2\text{dpma}$  to form  $\text{Zr}(\text{dpma})_2$  (**5**). Treatment of  $\text{Hf}(\text{NMe}_2)_4$  with 1 equiv of  $\text{H}_2\text{dpma}$  proceeds directly to  $\text{Hf}(\text{dpma})_2$  (**6**) replacing all four dimethylamido substituents. At present, we have not isolated a  $\text{Hf}(\text{NMe}_2)_2(\text{NHMe}_2)(\text{dpma})$  complex through this route, indicative of the relatively high basicity and polarity of Hf– $\text{NMe}_2$  substituents.

Generation of pseudo-octahedral  $\text{Ti}(\text{dpma})_2$  (**4**) was accomplished through reaction of  $\text{TiCl}_4$  with  $\text{Li}_2\text{dpma}$ . Regardless of the stoichiometry employed,  $\text{Ti}(\text{dpma})_2$  was the only observed product, and no dihalo derivatives were isolated. <sup>14</sup>N NMR spectroscopic properties of **4–6** indicate discernible bonding differences to the pyrrolyl nitrogens of the *dpma* ligand with the more electronegative titanium center exhibit-

ing the strongest influence on the nitrogen lone pair. In fact, the pyrrolyl chemical shift tracks linearly with the electronegativities of the group-4 triad.

Reaction of 1 equiv of  $\text{Li}_2\text{dpma}$  with up to 8 equiv of  $\text{TiCl}_4$  does not yield a detectable  $\text{TiCl}_2(\text{dpma})$  derivative. Is the lack of dichloro product the result of a kinetic effect during the reaction, or is the dihalo dpma complex unstable relative to its disproportionation products,  $\text{TiCl}_4$  and  $\text{Ti}(\text{dpma})_2$ , even at low temperature? To answer this question and to access these potentially useful starting materials, we devised another route to dihalo dpma complexes using  $\text{Ti}(\text{NMe}_2)_2(\text{dpma})$  (**1**) as starting material. Reaction of **1** with excess  $\text{ClSiMe}_3$  results in the formation of  $\text{TiCl}_2(\text{dpma})$ , which is most readily purified as the THF adduct  $\text{TiCl}_2(\text{dpma})(\text{THF})$  (**10**). We have not observed  $\text{Ti}(\text{dpma})_2$  (**4**) during these reactions, which is consistent with formation of  $\text{Ti}(\text{dpma})_2$  being kinetically enabled during the  $\text{Li}_2\text{dpma}$  and  $\text{TiCl}_2(\text{dpma})$  reaction.

Finally, using typical synthetic strategies, we prepared several complexes such as  $\text{Ti}(\text{NMe}_2)(\text{I})(\text{dpma})$  (**8**),  $\text{Ti}(\text{OCH}_2\text{CF}_3)_2(\text{THF})(\text{dpma})$  (**11**), and  $\text{Ti}(\text{NMe}_2)(\text{CH}_2\text{SiMe}_3)(\text{dpma})$  (**9**) that will provide excellent starting points for future reactivity and synthesis investigations. In 5-coordinate complexes such as **1** and **9**, exchange of the monodentate substituents is often slow with these tridentate, dianionic ligands.<sup>11</sup>

Group-4 dpma complexes have proved to be a fruitful synthetic system, and members of this class of complexes are finding applications in catalysis.<sup>10</sup>

## Experimental Section

**General Considerations.** All manipulations were carried out in an MBraun drybox under a purified nitrogen atmosphere unless stated otherwise. Anhydrous ether was purchased from Columbus Chemical Industries, Inc., and freshly distilled from purple sodium benzophenone ketyl. Toluene was purchased from Spectrum Chemical Mfg. Corp. and purified by refluxing over molten sodium under nitrogen for at least 2 d. Pentane (Spectrum Chemical Mfg. Corp.), tetrahydrofuran (JADE Scientific), 1,2-dimethoxyethane (DME, Aldrich Chemical Co.), and benzene (EM Science) were distilled from purple sodium benzophenone ketyl. Dichloromethane (EM Science) and acetonitrile (Spectrum Chemical) were distilled from calcium hydride. Chlorobenzene was distilled from  $\text{P}_2\text{O}_5$ . Tetra-*n*-butylammonium triflate was purchased from Aldrich and was used as received. Deuterated solvents were dried over purple sodium benzophenone ketyl ( $\text{C}_6\text{D}_6$ ) or  $\text{P}_2\text{O}_5$  ( $\text{CDCl}_3$ ) and distilled under nitrogen.  $\text{Ti}(\text{NMe}_2)_2(\text{dpma})$  was prepared as previously reported.<sup>6</sup> Anhydrous 2,6-lutidinium iodide was prepared according to the literature procedure.<sup>22</sup> Other compounds were purchased from commercial sources. Liquids were distilled under purified nitrogen or in vacuo prior to use. Cobaltocene was purchased from Strem Chemical Co. and was sublimed prior to use.  $^1\text{H}$  and  $^{13}\text{C}$  spectra were recorded on a Varian Inova-300 or VXR-500 spectrometer.  $^1\text{H}$  and  $^{13}\text{C}$  assignments were confirmed with the use of two-dimensional  $^1\text{H}$ - $^1\text{H}$  and  $^{13}\text{C}$ - $^1\text{H}$  correlation NMR experiments when necessary. All spectra were referenced internally to residual protiosolvent ( $^1\text{H}$ ) or solvent ( $^{13}\text{C}$ ) resonances. Chemical shifts are quoted in ppm and coupling constants in Hz. Common coupling constants are not reported.  $^{14}\text{N}$  NMR spectra were collected on a VXR-500 spectrometer and are referenced to external neat  $\text{CH}_3$ -

$\text{NO}_2$ .  $^{14}\text{N}$  NMR spectra are also conveniently referenced to dissolved natural abundance  $^{14}\text{N}_2$ , which was invariably noticeable in our samples prepared under purified nitrogen, as  $-72$  ppm ( $\nu_{1/2} = 50$ – $80$  Hz) in  $\text{C}_6\text{D}_6$  versus neat nitromethane.  $^{14}\text{N}$  NMR spectra were deconvoluted using Varian software, and data reported are from the spectral deconvolutions.

$\text{Ti}(\text{NMe}_2)_4$ ,<sup>28</sup>  $\text{Zr}(\text{NMe}_2)_4$ ,<sup>28</sup> and  $\text{Hf}(\text{NMe}_2)_4$ <sup>29</sup> were prepared using slight modifications of the literature procedures. The reactions were carried out in an MBraun drybox under an atmosphere of purified nitrogen. A slurry of  $\text{LiNMe}_2$  in  $\text{Et}_2\text{O}$  was frozen in a liquid nitrogen cold well. The slurry was allowed to warm until it could be stirred, and then  $\text{MCl}_4$  was added as a solution in pentane ( $\text{M} = \text{Ti}$ ) or ether ( $\text{M} = \text{Zr}, \text{Hf}$ ). The reaction was allowed to warm and stir overnight. Volatiles were removed in vacuo. The product was extracted into pentane and filtered to remove salts. Final purification was accomplished by distilling ( $\text{M} = \text{Ti}$ ) or recrystallizing ( $\text{M} = \text{Zr}$  and  $\text{Hf}$ ).

**Procedure for Cyclic Voltammetry.** The electrochemical measurements were performed in 0.1 M tetra-*n*-butylammonium trifluoromethanesulfonate in chlorobenzene solution containing the compound of interest. In a typical experiment, 5–10 mg of the complex was dissolved in 10 mL of 0.1 M tetra-*n*-butylammonium trifluoromethanesulfonate solution. A Pt disk electrode and two silver wires were employed as working, auxiliary, and reference electrodes, respectively. All measurements were performed in a one-compartment cell. The electrochemical response was collected with the assistance of a CHI630A electrochemical analyzer made by CH Instruments. All of the potentials are reported versus the internally measured  $\text{FeCp}_2^{0/+}$  couple as 0.00 V.

**General Considerations for X-ray Diffraction.** Crystals grown at  $-35$  °C were moved quickly from a scintillation vial to a microscope slide containing Paratone N. Samples were selected and mounted on a glass fiber in wax and Paratone. The data collections were carried out at a sample temperature of 173(2) K on a Bruker AXS three-circle goniometer with a CCD detector. The data were processed and reduced utilizing the program SAINTPLUS supplied by Bruker AXS. The structures were solved by direct methods (SHELXTL v5.1, Bruker AXS) in conjunction with standard difference Fourier techniques. The figures shown were produced using ORTEP, and ellipsoids are at the 25% probability level.

***N,N*-Di(pyrrolyl- $\alpha$ -methyl)-*N*-methylamine ( $\text{H}_2\text{dpma}$ ).** This preparation is a modification of the literature procedure.<sup>8</sup> To a solution of methylamine hydrochloride (6.7 g, 99 mmol) in 100 mL of absolute ethanol in a 55 °C oil bath was added aqueous formaldehyde solution (37%, 16.2 g, 200 mmol). After most of the methylamine hydrochloride was dissolved, pyrrole (13.4 g, 200 mmol) was added to the reaction mixture. The resulting mixture was allowed to reflux at 55 °C for 4 h, and volatiles were removed under reduced pressure yielding a viscous oil. The oil was triturated with ether to give a white solid. The solid was then dissolved in water, basified with 5%  $\text{K}_2\text{CO}_3$ , and extracted with ether. Additional  $\text{K}_2\text{CO}_3$  was added, if necessary to bring the pH of the solution above 7, and the solution was extracted twice more with ether. The organic layers were combined, and volatiles were removed in vacuo. The resulting oil was crystallized from benzene/hexanes at  $-35$  °C yielding the product as a colorless solid. Yield: 13.7 g (72%).  $^1\text{H}$  NMR (300 MHz,  $\text{CDCl}_3$ ):  $\delta = 8.38$  (2 H, s, *N*(*H*)-pyrrole), 6.59 (2 H, m, 5- $\text{C}_4\text{H}_3\text{N}$ ), 6.01 (2 H, m, 4- $\text{C}_4\text{H}_3\text{N}$ ), 5.93 (2 H, m, 3- $\text{C}_4\text{H}_3\text{N}$ ), 3.37 (4 H, s,  $\text{C}_4\text{H}_3\text{NCH}_2\text{N}$ ), 2.07 (3 H, s,  $\text{C}_4\text{H}_3\text{NCH}_2\text{NMe}$ ).  $^{13}\text{C}$  NMR ( $\text{CDCl}_3$ ):  $\delta = 127.53$  (2- $\text{C}_4\text{H}_3\text{N}$ ), 117.95

(28) Bradley, D. C.; Thomas, I. M. *J. Chem. Soc.* **1960**, 3857–3861

(29) Chanda, G.; Lappert, M. F. *J. Chem. Soc. A* **1968**, 1940–1945.

(5- $C_4H_3N$ ), 108.50 (4- $C_4H_3N$ ), 107.86 (3- $C_4H_3N$ ), 53.37 ( $C_4H_3NCH_2N$ ), 41.52 (dpma-NMe).  $^{14}N$  NMR ( $C_6D_6$ ):  $\delta = -234$  ( $\nu_{1/2} = 1160$  Hz).

**Zr(NMe<sub>2</sub>)<sub>2</sub>(NHMe<sub>2</sub>)(dpma) (2).** To a 0 °C solution of Zr(NMe<sub>2</sub>)<sub>4</sub> (1.42 g, 5.31 mmol) in ether (5 mL) was added dropwise H<sub>2</sub>dpma (1.01 g, 5.31 mmol) in ether (5 mL). The reaction mixture was allowed to warm to room temperature and stirred 16 h. The product precipitated as a colorless solid, which was collected by filtration and dried in vacuo. The product was purified by recrystallization from toluene at -35 °C. Yield: 1.63 g (75%).  $^1H$  NMR (300 MHz,  $C_6D_6$ ):  $\delta = 7.07$  (2 H, s, 5- $C_4H_3N$ ), 6.57 (2 H, m, 4- $C_4H_3N$ ), 6.24 (2 H, s, 3- $C_4H_3N$ ), 3.72 (2 H, d,  $^2J = 13.4$  Hz,  $C_4H_3NCH_2N$ ), 3.22 (2 H, d,  $^2J = 13.9$  Hz,  $C_4H_3NCH_2N$ ), 3.11–2.40 (13 H, m, (NMe<sub>2</sub>)<sub>2</sub>(NHMe<sub>2</sub>)), 2.09 (3 H, s, NCH<sub>3</sub>), 1.69 (6 H, d, NMe<sub>2</sub>).  $^{13}C$  NMR ( $C_6D_6$ ):  $\delta = 137.5$  (2- $C_4H_3N$ ), 125.8 (5- $C_4H_3N$ ), 109.7 (4- $C_4H_3N$ ), 105.0 (3- $C_4H_3N$ ), 59.0 ( $C_4H_3NCH_2N$ ), 44.5 (NMe<sub>2</sub>), 42.6 (NHMe<sub>2</sub>), 38.7 (NCH<sub>3</sub>). Elemental analysis for ZrC<sub>17</sub>H<sub>32</sub>N<sub>6</sub>, found (calculated): C, 49.23 (49.61); H, 7.63 (7.78); N, 20.00 (20.43).

**Zr(NMe<sub>2</sub>)<sub>2</sub>(pyridine)(dpma) (3).** To a 0 °C solution of Zr(NMe<sub>2</sub>)<sub>2</sub>(NHMe<sub>2</sub>)(dpma) (293 mg, 0.71 mmol) in benzene (5 mL) was added pyridine (200 mg, 2.53 mmol) in benzene (5 mL). The reaction mixture was stirred at room temperature for 16 h after which time volatiles were removed under reduced pressure. The product crystallized from CH<sub>2</sub>Cl<sub>2</sub> at -35 °C as a colorless solid. Yield: 260 mg (82%).  $^1H$  NMR (300 MHz, CDCl<sub>3</sub>):  $\delta = 7.65$  (2 H, m, 2,6-pyridine), 7.46 (2 H, m, 3,5-pyridine), 7.13 (2 H, s, 5- $C_4H_3N$ ), 6.67 (1 H, m, 4-pyridine), 6.33 (2 H, m, 4- $C_4H_3N$ ), 6.25 (2 H, s, 3- $C_4H_3N$ ), 3.44 (2 H, d,  $^2J = 14$  Hz,  $C_4H_3NCH_2N$ ), 3.28 (2 H, d,  $^2J = 14$  Hz,  $C_4H_3NCH_2N$ ), 2.99 (6H, s, NMe<sub>2</sub>), 2.83 (6 H, s, NMe<sub>2</sub>), 2.28 (3 H, s, NCH<sub>3</sub>).  $^{13}C$  NMR (CDCl<sub>3</sub>):  $\delta = 150.6$  (2,6-pyridine), 138.9 (3,5-pyridine), 138.2 (2- $C_4H_3N$ ), 126.1 (4-pyridine), 124.8 (5- $C_4H_3N$ ), 108.7 (4- $C_4H_3N$ ), 104.4 (3- $C_4H_3N$ ), 60.3 ( $C_4H_3NCH_2N$ ), 45.5 (NMe<sub>2</sub>), 44.4 (NMe<sub>2</sub>), 43.1 (NCH<sub>3</sub>). Elemental analysis for ZrC<sub>20</sub>H<sub>30</sub>N<sub>6</sub>, found (calculated): C, 53.76 (53.90); H, 6.47 (6.74); N, 18.27 (18.87).

**Ti(dpma)<sub>2</sub> (4).** To TiCl<sub>4</sub> (2.62 g, 13.8 mmol) in toluene (15 mL) cooled to -90 °C was added solid Li<sub>2</sub>dpma (5.55 g, 27.6 mmol). The reaction mixture was allowed to stand at -35 °C for 48 h after addition. The resulting black solution was filtered, and volatiles were removed in vacuo yielding a black solid. The solid was dissolved into CH<sub>2</sub>Cl<sub>2</sub> and concentrated by room-temperature evaporation into toluene to give Ti(dpma)<sub>2</sub> as black blocks. Yield: 1.48 mg (25%).  $^1H$  NMR (300 MHz, CDCl<sub>3</sub>):  $\delta = 7.41$  (2 H, d, 5- $C_4H_3N$ ), 6.11 (2 H, d, 5'- $C_4H_3N$ ), 6.03 (2 H, dd, 4- $C_4H_3N$ ), 5.92 (4 H, m, 3,3'- $C_4H_3N$ ), 5.79 (2 H, dd, 4'- $C_4H_3N$ ), 4.53 (2 H, d,  $^2J = 14$  Hz,  $C_4H_3NCH_2N$ ), 4.07 (2 H, d,  $^2J = 14$  Hz,  $C_4H_3NCH_2N$ ), 3.91 (2 H, d,  $^2J = 14.4$  Hz,  $C_4H_3NCH_2N$ ), 3.49 (2H, d,  $^2J = 13.7$  Hz,  $C_4H_3NCH_2N$ ), 2.28 (6 H, s,  $C_4H_3NCH_2NMe$ ).  $^{13}C$  NMR (CDCl<sub>3</sub>):  $\delta = 138.9$  (2- $C_4H_3N$ ), 136.8 (2'- $C_4H_3N$ ), 129.5 (5- $C_4H_3N$ ), 129.3 (5'- $C_4H_3N$ ), 107.6 (4- $C_4H_3N$ ), 107.5 (4'- $C_4H_3N$ ), 105.0 (3- $C_4H_3N$ ), 103.4 (3'- $C_4H_3N$ ), 59.9 ( $C_4H_3NCH_2N$ ), 59.3 ( $C_4H_3NCH_2N$ ), 47.5 (dpma-NMe).  $^{14}N$  NMR ( $C_6D_6$ ):  $\delta = -84$  (pyrrolyl,  $\nu_{1/2} = 1238$  Hz), -239 (MeN,  $\nu_{1/2} = 553$  Hz). UV-vis: 384 nm ( $\epsilon = 15682$  cm<sup>-1</sup> M<sup>-1</sup>). Cyclic voltammogram [chlorobenzene, 100 mV/s]: -1.26 V (rev). Elemental analysis for TiC<sub>22</sub>H<sub>26</sub>N<sub>6</sub>, found (calculated): C, 63.22 (62.53); H, 6.35 (6.16); N, 19.16 (19.89).

**[CoCp<sub>2</sub>][Ti(dpma)<sub>2</sub>] (7).** To Ti(dpma)<sub>2</sub> (123 mg, 0.29 mmol) in THF (5 mL) cooled to near frozen was added CoCp<sub>2</sub> (55 mg, 0.29 mmol) in THF dropwise. The addition produced a brown precipitate. Further stirring for 1 h followed by filtration afforded the product as a brown solid. Yield: 88 mg (49%). Magnetic

susceptibility (Evans' method):  $\mu_{\text{eff}} = 2.05 \mu_B$ . Elemental analysis for C<sub>32</sub>H<sub>36</sub>CoN<sub>6</sub>Ti, found (calculated): C, 61.92 (62.86); H, 5.96 (5.93); N, 13.22 (13.94).

**Zr(dpma)<sub>2</sub> (5).** To a 0 °C solution of Zr(NMe<sub>2</sub>)<sub>2</sub>(NHMe<sub>2</sub>)(dpma) (334 mg, 0.81 mmol) in benzene (5 mL) was added a colorless solution of H<sub>2</sub>dpma (153 mg, 0.81 mmol) in benzene (5 mL) dropwise. The reaction mixture was stirred at room temperature for 16 h after which time volatiles were removed under reduced pressure to give a yellow solid. The solid was recrystallized from CH<sub>2</sub>Cl<sub>2</sub> at -35 °C. Yield: 254 mg (67%).  $^1H$  NMR (300 MHz,  $C_6D_6$ ):  $\delta = 7.21$  (2 H, d, 5- $C_4H_3N$ ), 6.51 (2 H, d, 5'- $C_4H_3N$ ), 6.24 (2 H, dd, 4- $C_4H_3N$ ), 6.17 (2 H, dd, 4'- $C_4H_3N$ ), 6.09 (2 H, d, 3- $C_4H_3N$ ), 6.04 (2 H, d, 3'- $C_4H_3N$ ), 4.06 (2 H, d,  $^2J = 14$  Hz,  $C_4H_3NCH_2N$ ), 3.47 (2 H, d,  $^2J = 14.2$  Hz,  $C_4H_3NCH_2N$ ), 3.15 (2 H, d,  $^2J = 14$  Hz,  $C_4H_3NCH_2N$ ), 2.83 (2 H, d,  $^2J = 13.7$  Hz,  $C_4H_3NCH_2N$ ), 2.02 (6 H, s, NCH<sub>3</sub>).  $^{13}C$  NMR ( $C_6D_6$ ):  $\delta = 138.0$  (2- $C_4H_3N$ ), 135.9 (2'- $C_4H_3N$ ), 128.5 (5- $C_4H_3N$ ), 128.5 (5'- $C_4H_3N$ ), 110.2 (4- $C_4H_3N$ ), 110.2 (4'- $C_4H_3N$ ), 108.0 (3- $C_4H_3N$ ), 106.2 (3'- $C_4H_3N$ ), 58.8 ( $C_4H_3NCH_2N$ ), 57.7 ( $C_4H_3NCH_2N$ ), 47.1 (NCH<sub>3</sub>).  $^{14}N$  NMR ( $C_6D_6$ ):  $\delta = -128$  (pyrrolyl,  $\nu_{1/2} = 1365$  Hz), -240 (MeN,  $\nu_{1/2} = 296$  Hz). Cyclic voltammogram [chlorobenzene, 100 mV/s]: -1.41 V (irr). Elemental analysis for C<sub>22</sub>H<sub>26</sub>N<sub>6</sub>Zr, found (calculated): C, 56.56 (56.75); H, 5.73 (5.63); N, 17.62 (18.05).

**Hf(dpma)<sub>2</sub> (6).** To a 0 °C solution of Hf(NMe<sub>2</sub>)<sub>4</sub> (316 mg, 0.89 mmol) in benzene (5 mL) was added H<sub>2</sub>dpma (337 mg, 1.78 mmol) in benzene (5 mL) dropwise. The reaction mixture was stirred at room temperature for 16 h after which time volatiles were removed under reduced pressure to give a brown solid. The product was recrystallized from CH<sub>2</sub>Cl<sub>2</sub> at -35 °C. Yield: 374 mg (75%).  $^1H$  NMR (300 MHz, CDCl<sub>3</sub>):  $\delta = 7.11$  (2 H, d, 5- $C_4H_3N$ ), 6.24 (2 H, d, 5'- $C_4H_3N$ ), 6.15 (4 H, m, 4,4'- $C_4H_3N$ ), 6.07 (2 H, m, 3- $C_4H_3N$ ), 5.99 (2 H, m, 3'- $C_4H_3N$ ), 4.43 (2 H, d,  $^2J = 14$  Hz,  $C_4H_3NCH_2N$ ), 4.16 (2 H, d,  $^2J = 14$  Hz,  $C_4H_3NCH_2N$ ), 3.95 (2 H, d,  $^2J = 14.2$  Hz,  $C_4H_3NCH_2N$ ), 3.62 (2 H, d,  $^2J = 13.7$  Hz,  $C_4H_3NCH_2N$ ), 2.57 (6 H, s, NCH<sub>3</sub>).  $^{13}C$  NMR (CDCl<sub>3</sub>):  $\delta = 137.4$  (2- $C_4H_3N$ ), 136.2 (2'- $C_4H_3N$ ), 128.6 (5- $C_4H_3N$ ), 128.3 (5'- $C_4H_3N$ ), 110.4 (4- $C_4H_3N$ ), 110.2 (4'- $C_4H_3N$ ), 107.8 (3- $C_4H_3N$ ), 106.4 (3'- $C_4H_3N$ ), 59.2 ( $C_4H_3NCH_2N$ ), 58.0 ( $C_4H_3NCH_2N$ ), 47.6 (NCH<sub>3</sub>).  $^{14}N$  NMR ( $C_6D_6$ ):  $\delta = -131$  (pyrrolyl,  $\nu_{1/2} = 1586$  Hz), -239 (MeN,  $\nu_{1/2} = 425$  Hz). Cyclic voltammogram [chlorobenzene, 100 mV/s]: -1.57 V (irr). Elemental analysis for C<sub>22</sub>H<sub>26</sub>HfN<sub>6</sub>, found (calculated): C, 47.94 (47.76); H, 4.92 (4.70); N, 15.12 (15.20).

**Ti(NMe<sub>2</sub>)(CH<sub>2</sub>SiMe<sub>3</sub>)(dpma) (9).** To a solution of Ti(I)(NMe<sub>2</sub>)(dpma) (272 mg, 0.67 mmol) in DME (5 mL) and dioxane (2 mL) cooled to near frozen was added a solution of Me<sub>3</sub>SiCH<sub>2</sub>MgCl (804  $\mu$ L, 0.80 mmol, 1.0 M solution in ether) in ether/DME (5 mL) dropwise. The reaction mixture was allowed to warm to room temperature and stirred 1 h resulting in the formation of a white precipitate. The precipitate was filtered away, and the filtrate was pumped dry yielding a yellow solid. Fractional crystallization from pentane allowed separation of two isomers of Ti(NMe<sub>2</sub>)(CH<sub>2</sub>SiMe<sub>3</sub>)(dpma). Yield: **9a**, 87 mg (35%); **9b**, 59 mg (24%). Elemental analysis for C<sub>17</sub>H<sub>30</sub>N<sub>4</sub>SiTi mixture of isomers, found (calculated): C, 55.05 (55.73); H, 8.23 (8.25); N, 14.72 (15.29). Data for Ti-(axial-NMe<sub>2</sub>)(equatorial-CH<sub>2</sub>SiMe<sub>3</sub>)(dpma) **9a**.  $^1H$  NMR (300 MHz,  $C_6D_6$ ): 7.18 (2 H, s, 5- $C_4H_3N$ ), 6.45 (2 H, m, 4- $C_4H_3N$ ), 6.18 (2 H, s, 3- $C_4H_3N$ ), 4.04 (2 H, d,  $^3J = 13.4$  Hz,  $C_4H_3NCH_2N$ ), 3.25 (2 H, d,  $^3J = 13.4$  Hz,  $C_4H_3NCH_2N$ ), 3.01 (6 H, m, NMe<sub>2</sub>), 1.98 (2 H, s, CH<sub>2</sub>SiMe<sub>3</sub>), 1.73 (3 H, s,  $C_4H_3NCH_2N(CH_3)$ ), -0.12 (9 H, s, CH<sub>2</sub>SiMe<sub>3</sub>).  $^{13}C$  NMR ( $C_6D_6$ ): 138.2 (2- $C_4H_3N$ ), 127.2 (5- $C_4H_3N$ ), 108.6 (4- $C_4H_3N$ ), 103.5 (3- $C_4H_3N$ ), 97.9 (CH<sub>2</sub>SiMe<sub>3</sub>), 59.8 ( $C_4H_3NCH_2N$ ), 46.0 (NMe<sub>2</sub>), 44.2 ( $C_4H_3NCH_2N(CH_3)$ ), 1.2 (CH<sub>2</sub>-SiMe<sub>3</sub>). Data for Ti(equatorial-NMe<sub>2</sub>)(axial-CH<sub>2</sub>SiMe<sub>3</sub>)(dpma) **9b**.



$^1\text{H}$  NMR (300 MHz,  $\text{C}_6\text{D}_6$ ): 7.13 (2 H, s, 5- $\text{C}_4\text{H}_3\text{N}$ ), 6.37 (2 H, m, 4- $\text{C}_4\text{H}_3\text{N}$ ), 6.07 (2 H, s, 3- $\text{C}_4\text{H}_3\text{N}$ ), 3.55 (2 H, d,  $^3J = 13.7$  Hz,  $\text{C}_4\text{H}_3\text{NCH}_2\text{N}$ ), 3.33 (2 H, d,  $^3J = 13.7$  Hz,  $\text{C}_4\text{H}_3\text{NCH}_2\text{N}$ ), 3.08 (6 H, m,  $\text{NMe}_2$ ), 2.20 (3 H, s,  $\text{C}_4\text{H}_3\text{NCH}_2\text{N}(\text{CH}_3)$ ), 1.88 (2 H, s,  $\text{CH}_2\text{-SiMe}_3$ ), 0.02 (9 H, s,  $\text{CH}_2\text{SiMe}_3$ ).  $^{13}\text{C}$  NMR ( $\text{C}_6\text{D}_6$ ): 137.5 (2- $\text{C}_4\text{H}_3\text{N}$ ), 127.0 (5- $\text{C}_4\text{H}_3\text{N}$ ), 108.8 (4- $\text{C}_4\text{H}_3\text{N}$ ), 103.9 (3- $\text{C}_4\text{H}_3\text{N}$ ), 93.3 ( $\text{CH}_2\text{SiMe}_3$ ), 58.2 ( $\text{C}_4\text{H}_3\text{NCH}_2\text{N}$ ), 47.1 ( $\text{NMe}_2$ ), 46.0 ( $\text{C}_4\text{H}_3\text{NCH}_2\text{N}(\text{CH}_3)$ ), 2.2 ( $\text{CH}_2\text{SiMe}_3$ ).

**TiCl<sub>2</sub>(THF)(dpma) (10).** To  $\text{ClSiMe}_3$  (5 mL, 39.4 mmol, 25 equiv) in THF (5 mL) was added solid  $\text{Ti}(\text{NMe}_2)_2(\text{dpma})$  (500 mg, 1.55 mmol). The resulting black mixture was stirred overnight, and volatiles were removed in vacuo to give a black solid. The solid was recrystallized from  $\text{CH}_2\text{Cl}_2/\text{pentane}$ . Yield: 302 mg (52%).  $^1\text{H}$  NMR (300 MHz,  $\text{CDCl}_3$ ):  $\delta = 7.54$  (2 H, s, 5- $\text{C}_4\text{H}_3\text{N}$ ), 5.84 (4 H, m, 3,4- $\text{C}_4\text{H}_3\text{N}$ ), 4.34 (1 H, s,  $^2J = 14$  Hz,  $\text{C}_4\text{H}_3\text{NCH}_2\text{N}$ ), 4.05 (1 H, s,  $^2J = 14$  Hz,  $\text{C}_4\text{H}_3\text{NCH}_2\text{N}$ ), 3.47 (4 H, s, 2- $\text{C}_4\text{H}_8\text{O}$ ), 2.80 (3 H, s,  $\text{NCH}_3$ ), 1.90 (4 H, s, 3- $\text{C}_4\text{H}_8\text{O}$ ).  $^{13}\text{C}$  NMR ( $\text{CDCl}_3$ ):  $\delta = 140.1$  (2- $\text{C}_4\text{H}_3\text{N}$ ), 131.6 (5- $\text{C}_4\text{H}_3\text{N}$ ), 106.5 (4- $\text{C}_4\text{H}_3\text{N}$ ), 102.9 (3- $\text{C}_4\text{H}_3\text{N}$ ), 72.7 (2- $\text{OC}_4\text{H}_8$ ), 61.6 ( $\text{C}_4\text{H}_3\text{NCH}_2\text{N}$ ), 50.4 ( $\text{NCH}_3$ ), 25.0 (3- $\text{OC}_4\text{H}_8$ ). Elemental analysis for  $\text{C}_{15}\text{H}_{21}\text{ON}_3\text{Cl}_2\text{Ti}$ , found (calculated): C, 47.18 (47.66); H, 5.56 (5.55); N, 11.02 (11.12).

**Ti(OCH<sub>2</sub>CF<sub>3</sub>)<sub>2</sub>(THF)(dpma) (11).** To a colorless solution of  $\text{TiCl}_2(\text{OCH}_2\text{CF}_3)_2$  (1 g, 3.16 mmol) in 5 mL of  $\text{Et}_2\text{O}$  chilled to  $-100$  °C was added a solution of  $\text{Li}_2\text{dpma}$  (634 mg, 3.16 mmol) in 5 mL of  $\text{Et}_2\text{O}$  dropwise. After stirring at room temperature for 1 h, a precipitate formed. The solution was filtered, and the volatiles were removed in vacuo from the filtrate. THF (406  $\mu\text{L}$ ) was added

to the resulting brown slurry. The product was dissolved in 3 mL of pentane and recrystallized at  $-35$  °C. Yield: 737 mg (46%).  $^1\text{H}$  NMR (300 MHz,  $\text{C}_6\text{D}_6$ ):  $\delta = 7.13$  (2 H, s, 5- $\text{C}_4\text{H}_3\text{N}$ ), 6.22 (2 H, s, 4- $\text{C}_4\text{H}_3\text{N}$ ), 5.94 (2 H, s, 3- $\text{C}_4\text{H}_3\text{N}$ ), 4.13 (4 H, m,  $\text{OCH}_2\text{CF}_3$ ), 3.57 (2 H, d,  $^2J = 13.6$  Hz,  $\text{C}_4\text{H}_3\text{NCH}_2\text{N}$ ), 3.52 (4 H, s, 2- $\text{C}_4\text{H}_8\text{O}$ ), 3.29 (2 H, d,  $^2J = 13.9$  Hz,  $\text{C}_4\text{H}_3\text{NCH}_2\text{N}$ ), 2.24 (3 H, s,  $\text{NCH}_3$ ), 1.33 (4 H, s, 3- $\text{C}_4\text{H}_8\text{O}$ ).  $^{13}\text{C}$  NMR ( $\text{C}_6\text{D}_6$ ):  $\delta = 138.1$  (2- $\text{C}_4\text{H}_3\text{N}$ ), 127.1 (5- $\text{C}_4\text{H}_3\text{N}$ ), 108.6 (4- $\text{C}_4\text{H}_3\text{N}$ ), 104.1 (3- $\text{C}_4\text{H}_3\text{N}$ ), 72.7 (2- $\text{OC}_4\text{H}_8$ ), 68.0 ( $\text{OCH}_2\text{CF}_3$ ), 58.9 ( $\text{C}_4\text{H}_3\text{NCH}_2\text{N}$ ), 47.3 ( $\text{NCH}_3$ ), 25.6 (3- $\text{OC}_4\text{H}_8$ ). Elemental analysis for  $\text{C}_{19}\text{H}_{25}\text{F}_6\text{N}_3\text{O}_3\text{Ti}$ , found (calculated): C, 44.41 (45.10); H, 4.94 (4.99); N, 8.23 (8.32).

**Acknowledgment.** The authors thank Petroleum Research Fund (38376-AC3), the Department of Energy Defense Programs (27856-001-01 38), and Michigan State University for financial support. A.L.O. is an Office of Naval Research Young Investigator (N00014-01-1-0638). J.T.C. thanks Michigan State University for a Brubaker Fellowship.

**Supporting Information Available:** Tables from X-ray diffraction studies on **2**, **4**, **5**, **6**, **7**, **9**, **10**, and **11**. Cyclic voltammograms on **4**, **5**, and **6**.  $^{14}\text{N}$  NMR spectra for  $\text{H}_2\text{dpma}$ , **4**, **5**, and **6** including spectral fits. Representative  $^1\text{H}$  NMR spectra of **4**, **9**, and **11**. This material is available free of charge via the Internet at <http://pubs.acs.org>.

IC0259484